Conf-761008--1

LA-UR -76-1672

TITLE: PRELIMINARY ASSESSMENT OF A GEOTHERMAL ENERGY RESERVOIR FORMED BY HYDRAULIC FRACTURING

AUTHOR(S): Hugh D. Murphy, Robert G. Lawton, Jefferson W. Tester, Robert M. Potter, Donald W. Brown and R. Lee Aamodt

SUBMITTED TO: Society of Petroleum Engineers' 51 Annual Meeting, New Orleans, October 3-6, 1976

MASTER

los alamos scientific laboratory
of the University of California
LOS ALAMOS, NEW MEXICO 87545

An Affirmative Action/Equal Opportunity Employer

DISTRIBUTION OF THIS DOCUMENT IS UNLIMITED

Form No. 836
St. No. 2629
1/75

UNITED STATES
ENERGY RESEARCH AND
DEVELOPMENT ADMINISTRATION
CONTRACT W-7405-ENG. 36

DISCLAIMER

N A

60

ABSTRACT:

Two, 3-km-deep boreholes have been drilled into hot (∿ 200°C) granite in northern New Mexico in order to extract geothermal energy from hot dry rock. Both boreholes were hydraulically fractured to establish a flow connection. Presently this connection has a large flow impedance which may be improved with further stimulation. Fracture-to-borehole intersection locations and in situ thermal conductivity were determined from flowing temperature logs. In situ measurements of permeability show an extremely strong dependance upon pore pressure -- the permeability increased by a factor of 80 as the pressure was increased 83 bars (1200 psi). An estimate of the minimum horizontal earth stress was derived from fracture extension pressures and found to be one-half the overburden stress.

INTRODUCTION:

A program designed to demonstrate the feasibility of extracting energy from hot dry rock has been initiated at the Los Alamos Scientific Laboratory. Basically, it is proposed that man-made geothermal energy reservoirs can be created by drilling into relatively impermeable rock to a depth where the temperature is high enough to be useful; creating a reservoir by hydraulic fracturing; and then completing the circulation loop by drilling a second hole to intersect the hydraulically fractured region, or by drilling into the immediate vicinity of the first fracture and then creating a second fracture that intersects the first one.

References and illustrations at end of paper

Thermal power would be extracted from this system by injecting cold water down the first hole, forcing the water to sweep by the freshly exposed hot rock surface in the reservoir/fracture system, and then returning the hot water to the surface where the thermal energy would be converted to electrical energy or used for other purposes. System pressures would be maintained such that only one phase, liquid water, would be present in the reservoir and the drilled holes. The concept is described in more detail by Smith, et al[1] and the mechanics of the heat extraction process have been reported by Harlow and Pracht,[2] and McFarland and Murphy.[3]

The hot dry rock concept is being investigated in a series of field experiments at a site called Fenton Hill, located on the west flank of a dormant volcano, the Valles Caldera, in the Jemez mountains of northern New Mexico. In December 1974, the first deep borehole, GT-2, was completed to a depth of 2.929 km (9609 ft) in granite, where the temperature was 197°C (386°F). A hydraulic fracture was then created close to the bottom of this borehole. A second borehole, EE-1, was then drilled to complete the circulation loop, but it failed to intersect the GT-2 fracture by approximately 6 m (20 ft). Communication between the wellbores was then established by initiating a fracture from EE-1. This fracture is located an average distance of approximately 6 m (20 ft) from the GT-2 fracture. Due to uncertainties in fracture orientation measurements, it is not known whether the two fractures intersect. A series of flow experiments was then conducted to determine the nature of this circulation path, and to measure fracture properties necessary to complete the design of a demonstration heat extraction experiment. The results of these experiments are described in the following sections.

ANALYSIS OF TRANSIENT WELLBORE PRESSURES:

By assuming constant, one-dimensional, permeable flow into a homogeneous porous media with constant properties, and by also assuming that the hydraulic conductivity of the fracture is very large compared to that of the rock, it can be shown that if water is injected into a fracture at a constant rate, q, the change in fracture pressure, P, is:[4,5]

$$P = \frac{2\mu q}{kA}\sqrt{\frac{\kappa t}{\pi}} \quad \ldots\ldots\ldots\ldots \quad (1)$$

Because the hydraulic diffusivity, κ, is

$$\kappa = k/\mu\,\bar{\beta} \quad \ldots\ldots\ldots\ldots \quad (2)$$

the product of the fracture area times the square root of permeability, $A\sqrt{k}$, is given by rewriting Eq 1.

$$A\sqrt{k} = 2\sqrt{\frac{\mu}{\pi\bar{\beta}}}\;\frac{q\sqrt{t}}{P} \quad \ldots\ldots\ldots \quad (3)$$

Downhole pressure changes at the fracture face are estimated by correcting the measured surface wellhead pressure for pressure losses. These pressure losses consist of frictional losses in surface piping, flowing friction in the wellbore and, as the flow enters the fracture, an additional wellbore-to-fracture impedance (analogous to a skin effect). Since the flow rate is constant and wellbore storage effects are not significant, the total pressure loss due to these effects is also constant, and can be estimated by extrapolating the pressure curves back to zero time.

Typical data for the EE-1 fracture are presented in Figure 1. The experiment was conducted by pumping into the EE-1 wellbore at a constant rate of 2.1 ℓ/s (34 gal/min), corrected to downhole conditions. A good linear fit to the data is obtained on P versus $\sqrt{t}$ coordinates. Deviation of the later time data from the linear fit is thought to be due to pressure dependent permeability, or a "leak" from the EE-1 fracture to the GT-2 fracture via a flow connection; as will be discussed.

Since the porosity of the granite is less than 1%, the mean compressibility, $\bar{\beta}$, is essentially that of the rock which, based upon the results of sonic velocity logs, is estimated to be 2.7×10^{-6} bar^{-1} (1.9×10^{-7} psi^{-1}; 1 bar = 10^5 N/m^2 = 14.5 psi). Using available properties of water at 200°C,[6] and the above values of $\bar{\beta}$ and q, it can be shown that the $A\sqrt{k}$ value for the EE-1 fracture at the time this experiment was conducted was 2.2×10^{-5}m^3 (7.8×10^{-4} cu ft). Since this result was obtained with an initial pore pressure of zero (taking hydrostatic pressure as the baseline), the $A\sqrt{k}$ derived is more properly designated as $(A\sqrt{k})_o$, where the subscript represents the change in the initial pore pressure.

An extrapolation of the linear fit in Fig. 1 back to zero time provides an estimate of 2.8 bars (40 psi) for the pressure losses between the surface and the fracture. Although this pressure loss is probably not linear with flow rate, especially at much higher flow rates, it is instructive, for purposes of comparison, to divide it by the flow rate to yield a specific impedance. This specific impedance from the surface to the EE-1 fracture is 1.3 bar-sec/liter (1.2 psi-min/gal) which, as we will show, is small compared to the overall circulation impedance. Similar results with the GT-2 fracture indicate that its $(A\sqrt{k})_o$ is 5.2×10^{-5}m^3 (1.8×10^{-3} cu ft) and the surface to GT-2 fracture impedance is 3.9 bar-sec/liter (3.5 psi-min/gal). Potter et al[7] report that the permeability of GT-2 core specimens is 0.01 to 0.1 micro-darcy at downhole conditions of temperature and pressure, while West et al[8] report that, based upon drill-stem testing at a depth of 1.5 km (5000 ft) in GT-2, the permeability of a similar granite is approximately one micro-darcy. Taking the latter result as perhaps more representative of heterogenous rock conditions suggests that the area of the GT-2 fracture is approximately 5.2×10^4m^2 (5.6×10^5 sq ft), and if circular, has a radius of 90 m (300 ft). This is a rough estimate of course, but Albright[9] reports, on the basis of microseismic acoustic techniques, that the radius of the GT-2 fracture must be at least 50 m (160 ft).

It is found that values of $(A\sqrt{k})_o$ are most useful when they are interpreted as a parameter which characterizes a fracture. Changes in $(A\sqrt{k})_o$ indicate irreversible changes in a fracture, examples being fracture extension due to pressurization or changes in k due to potential geochemical effects such as the formation and precipitation of rock-water interaction products or the dissolution of rock mineral components, particularly silica (SiO_2).

A historical summary of the $(A\sqrt{k})_o$ for both fractures is presented in Figure 2. At the top of this figure are identified the various flow experiments (which are discussed in more detail in reference 10), while near the bottom, the maximum EE-1 wellhead pressure achieved during each experiment is indicated. Since the creation of the EE-1 fracture in October, 1975, its $(A\sqrt{k})_o$ has increased during several of these flow experiments. Furthermore, these increases have been observed only when the EE-1 pressure has exceeded 90 to 94 bars (1300 to 1360 psi). Thus, it is believed that these increases in $(A\sqrt{k})_o$ are due to increases in A (fracture extensions) and that the fracture extension pressure, P_e, is approximately 92 bars (1330 psi) above hydrostatic. Since its creation, $(A\sqrt{k})_o$ of the GT-2 fracture has not changed significantly. The maximum sustained pressure ever reached at the GT-2 wellhead was 91 bars (1320 psi), i.e., below P_e. The permeability of the rock surrounding the GT-2 fracture has apparently not changed, in spite of the potential geochemical effects cited above.

DETERMINATION OF MINIMUM EARTH STRESS:

Based upon a theory of fracture mechanics, Sack[11] has shown that the difference between the fracture extension pressure and the earth stress perpendicular to the fracture plane, S_3, (the least compressive principal stress) is:

$$P_e - S_3 = \sqrt{\frac{\pi\gamma E}{2(1-\nu^2)R}} \quad . . . . \quad (4)$$

Aamodt[12] has reported values of the properties for a granite similar to that found in EE-1 and GT-2; $\gamma = 100$ J/m^2 (6.8 lb/ft), $E = 3.8 \times 10^5$ bars (5.5×10^6 psi) and $\nu = 0.3$. Substituting these values and supposing that either fracture radius, R, is presently as small as 50 m (160 ft), it can be shown that $P_e - S_3$ is only 3.6 bars (53 psi). Thus the minimum earth stress, S_3, in the EE-1 fracture is approximately 88 bars (1280 psi) above hydrostatic. As will be shown, the EE-1 fracture is roughly centered about a depth of 2.95 km (9670 ft), so that the absolute value of S_3 is 375 bars (5440 psi) or 50% of the overburden pressure, S_1, (the maximum compressive principal stress). As expected, these fractures are vertically oriented.

PORE PRESSURE DEPENDENT PERMEABILITY:

The effects of pore pressure upon $A\sqrt{k}$ are indicated in Figure 3. The results were obtained from an experiment (No. 111) in which the sequence of operations was to first inject water into the EE-1 fracture at a constant rate until a pressure of 28 bars (400 psi) above hydrostatic was reached, and then adjust the flow rate such that this pressure was maintained constant for two hours. In such a manner a new pore pressure was established in the rock adjacent to the fracture face. Following the two-hour "soak" the procedure was repeated at the additional pressure levels shown on the figure. The start of each new change in pressure level was taken as a new zero time and the results, when plotted versus $\sqrt{t}$, yielded straight lines as shown. Using a modified principle of superposition, the $A\sqrt{k}$ for each increment of pressure can be calculated and the results are indicated on the figure. As can be seen, increasing the pore pressure from 0 to 69 bars (1000 psi) above hydrostatic resulted in a factor of 3.8 increase in $A\sqrt{k}$. Since A did not change (pressure levels were below the fracture extension pressure) the permeability apparently increased by a factor of 15.

Additional results, obtained from another flow experiment (No. 114), presented in Figure 4 indicate that the permeability increases even more sharply (up to a factor of 80!) as the pore pressure increases to 83 bars (1200 psi) above hydrostatic. These results are qualitatively similar to those of Brace, et al[13] for westerly granite and to those of Potter, et al[7] for GT-2 core specimens. If one interprets the "effective" stress holding microcracks closed as simply the difference between the earth stress and the pore pressure, then Brace, et al[13] have shown that reducing the effective stress by increasing the pore pressure tends to open the microcracks, leading to large changes in the effective permeability of the rock.

Figure 5 presents a summary of all the data we have measured pertaining to pore-pressure-dependent permeability. Included are data from the EE-1 fracture, the present GT-2 fracture (roughly centered at 2.81 km) and an early, now-inactive fracture in GT-2. Empirically we have found that the square root of the ratio of the permeability at zero wellhead pressure to the permeability at elevated pressures, $\sqrt{k_o/k}$, is reasonably linear with pressure as shown. A value of zero for the ratio $\sqrt{k_o/k}$ at the intercept with the abscissa mathematically implies infinite permeability at the face of the fracture plane. A reasonable interpretation would be that when the pressure approaches the maximum horizontal component of earth stress, S_2, (the intermediate earth stress, aligned horizontally and parallel to the fracture plane) the effective stress in the S_2 direction approaches zero with concomitant opening of microfractures. The least squares line using the entire data set has the equation:

$$\sqrt{\frac{k_o}{k}} = 1.00 - 0.0098\ P(\text{Bars}) \quad . . . \quad (5)$$

and the extrapolated pressure, at $\sqrt{k_o/k} = 0$, of 102 bars (1480 psi) above hydrostatic is believed to be an estimate of S_2

ANALYSIS OF FLOWING TEMPERATURE LOGS:

In Situ Thermal Conductivity. The equation describing the heat transfer in the rock surrounding a wellbore is:

$$\frac{\partial^2 T}{\partial r^2} + \frac{1}{r}\frac{\partial T}{\partial r} = \frac{\rho c}{\lambda}\frac{\partial T}{\partial t} \quad . . . . \quad (6)$$

and the equation for the flowing fluid in the wellbore is:

$$\frac{\partial T_f}{\partial t} + U\frac{\partial T_f}{\partial z} = -\frac{2}{\rho_f c_f}\left(\frac{\lambda}{r}\frac{\partial T}{\partial r}\right)_{r = a} \quad . . \quad (7)$$

In the derivation of Eqs. 6 and 7 it has been assumed that the properties of the rock and the water are constant and that the turbulent mixing that occurs in the flowing water results in negligibly small radial temperature gradients in the water. If these equations are nondimensionalized, it can be shown[14] that a dimensionless temperature difference is a function of a dimensionless time and the ratio of the volumetric heat capacity of the rock to that of the fluid:

$$\frac{2\lambda\,(T_{of} - T_f)}{\rho_f c_f a^2 U \; dT_f/dz} = \Phi\left(\frac{\lambda t}{\rho\, c\, a^2}\right)\cdot \Psi\left(\frac{\rho c}{\rho_f c_f}\right) \quad . . . (8)$$

where T_f = fluid temperature at time t, depth z

T_{of} = initial fluid temperature at depth z

Equation 8 is valid when both the fluid velocity U, and the temperature gradient dT_f/dz do not vary significantly with time. The latter condition requires that the following dimensionless grouping be less than 0.3[14]

$$\rho_f c_f a U \sqrt{\alpha t}/\lambda z \leq 0.3 \quad . . . . (9)$$

A wellbore heat transmission computer program[15] was used to generate the functional form of Eq 8 for a value of $\rho c/\rho_f c_f$ appropriate for granite and 200°C water. The computed curve is shown in Fig. 6. This curve is essentially a type curve, and is the thermal analog to the type curve developed by Ramey[16] for pressure analysis of a single well in an infinite reservoir with wellbore storage.

All parameters except temperature and time, in Eq. 8, are assumed constant so if experimental values of log $(T_{of}-T_f)$ are plotted against log (t), the plot should have the same shape as Fig. 6. The data from the temperature logs taken in the GT-2 wellbore, at a depth of approximately 2.77 km (9100 ft), injecting at a constant rate of 0.6 liter/sec (9 gal/min) with conditions satisfying equation (9), were plotted on log-log coordinates and the results are overlayed on the type curve of Figure 6. A match of curve shape occurs and a match point at an experimental time of 10,000 seconds corresponds to a dimensionless time of 1.4. The wellbore radius is 0.087 m. Using a value of 2700 kg/m³ for the rock density, ρ, and a value of 1050 J/kg-K for the heat capacity c, the calculated value of the in situ thermal conductivity of the rock is 3.0 W/m-K (1.7 BTU/hr-ft-°F). This is in excellent agreement with the laboratory results reported by Sibbitt[17] for core specimens taken from GT-2.

As a check, the temperature difference at 10,000 seconds is 2.8°C and using values:

ρ_f = 950 kg/m³ (59.2 lb/ft³)

c_f = 4184 J/kg-K (1.0 BTU/lb-°F)

q = 6×10^{-4} m³/sec (9 gpm)

λ = 3.0 W/m-K (1.7 BTU/hr-ft-°F)

ΔT (dimensionless) = 0.66

a value of 32°C/km (0.017 °F/ft) is calculated for the average temperature gradient dT_f/dz. This is in excellent agreement with the local measured temperature log in the interval of the wellbore near 2.77 km (9100 ft). Average measured gradients from 1 to 2.9 km (3050 to 9600 ft) depths in GT-2 are between 50 and 60°C/km (0.027 and 0.032°F/ft).

Determination of Wellbore-to-Fracture Connection Depths. By assuming constant rock properties and a constant wellbore radius, the ratio of the water velocity U_2 (at some depth z_2 and time t) to the velocity U_1 at a reference depth z_1 is related to the water temperature changes and water temperature gradients, $\bar{G}$, at these depths and time as:

$$\frac{U_2}{U_1} = \frac{T_f(z_2) - T_{of}(z_2)}{T_f(z_1) - T_{of}(z_1)}\;\frac{\bar{G}\,(z_2)}{\bar{G}\,(z_1)} \quad . . . (10)$$

It should be noted that the gradient, $G = \partial T_f/\partial z$, is no longer required to be constant in Eq. 10 and in fact, the gradient to be used, $\bar{G}$, is an "effective average" gradient. For short time tests with insignificant wellbore heat storage ($1<\alpha t/a^2<10$), a useful approximation for $\bar{G}$ is:[14]

$$\bar{G} = \sqrt{G(t) \cdot \frac{1}{t}\int_0^t G(\tau)d\tau} \quad . . . . . (11)$$

The results of temperature logs taken while injecting at a constant rate into the GT-2 wellbore are shown in Figure 7. These logs were taken under conditions satisfying the short time criterion Eq. 9. The data of Figure 7 were analyzed per Eqs. (10) and (11) and Figure 8 presents the relative velocity as a function of depth. The depth intervals at which water is being lost to the surrounding rock are exceptionally well defined by this technique. Furthermore, Figure 8 indicates that 80% of the water is flowing into a fracture over a more narrow interval (∿ 40 m) than is suggested by the depression in the logs of Figure 7. The relative velocities plotted in the intervals where the relative velocity changes from 1.0 to 0.2 and 0.2 to 0.05 may not be significant, since in these intervals water is flowing into the rock formation, and the rock energy equation, Eq. 6, should therefore incorporate an additional convective mode of heat transfer.

From Figure 8 it appears that the main connection between the GT-2 borehole and fracture is centered at 2.81 km (9220 ft), with a secondary connection at 2.87 km (9420 ft). The main connection occurs where the casing was damaged while "milling out" a packer and the secondary connection occurs where the casing was jet-perforated. A similar analysis of flowing temperature logs taken in the EE-1 borehole indicates that it is connected to its fracture at 2.95 km (9670 ft). Attempts to determine these fracture-to-wellbore connection points with spinner surveys have been unsuccessful because of the high temperatures at these depths.

IMPEDANCE TO FLOW CIRCULATION:

The circulation of flow through the present downhole system is characterized by high impedance. Figure 9 presents results of an experiment in which water was injected into EE-1 while GT-2 was vented. Since buoyancy effects due to temperature differences are not important in short term experiments the net pressure difference is simply the EE-1 pressure; while the net, circulated flow is simply the flow rate measured at the surface outlet at the GT-2 wellbore As can be seen, a linear relationship exists between the pressure difference and the circulated flow (at least at these low flow rates and the slope of the line yields the specific impedance, which for this experiment was 142 bar-sec/liter (130 psi-min/gal).

The results of many flow circulation tests indicate that flow appears at the venting wellbore in two or more stages suggesting that two or more paths of communication exist between the fractures. In the first stage, flow appears at the venting wellbore less than ten minutes after the start of pumping into the other wellbore This response is so fast compared to the calculated response time for the low permeability granite between the two fractures, which are estimated to be 6 m (20 ft) apart, that we conclude that this early-stage of flow must be via a set of natural fissures, or a zone of locally very high permeability, or even possibly by means of an intersection of the two hydraulic fractures.

Following this early-arriving flow, a slowly increasing flow rate is observed, possibly caused by permeation of water through the rock separating the two hydraulic fractures. As expected, this additional increment of flow rate varies with time and the pressure levels at the two boreholes as well as the size of the fractures. Because permeability so greatly increases with pore pressure, (see Figure 4) this second path of communication controls the major flow fraction,particularly for long-term tests where both wellbores are pressurized to high levels.

Figure 10 summarizes the impedance data to date. The circled data points represent the initial (first stage) impedance while the vertical bars represent the full range of transient impedance exhibited during each long-term test.

Anomalous transient pressure curves obtained during experiments 102 and 106 suggest that the declines in initial impedance observed during these experiments are due to the removal of impedances in the fractures; possibly a "flushing out" of rock/water/drilling fluid interaction products which had partially closed the fractures to flow.

Figure 10 indicates that the lowest impedance measured to date is approximately 28 bar-sec/liter (25 psi-min/gal). Because of uncertainties in the area of overlap of the two fractures, and the distance between the two fractures, and the extreme variation of permeability with pore pressure, it is difficult to estimate the minimum value of impedance attainable with the present system. However, very approximate calculations suggest that if both boreholes were maintained at 90 bars (1300 psi), i.e., slightly below P_e, the impedance of the rock between the two fractures might ultimately drop to 5 bar-sec/liter (5 psi-min/gal), i.e., comparable to the other impedances in the system.

DISCUSSION:

System Potential As A Demonstration Heat Extraction Experiment. The measured *in situ* permeability, even at high pressures is low enough that "leak off," requiring the continuous replenishment of water to the system, is not a serious problem. Both fractures appear to be located deep enough so that their temperatures should exceed 185°C (364°F). At the present time both fractures have a computed radius of 90 m (300 ft) or more. The *in situ* thermal conductivity is 3 W/mK, which is as high as can be expected from competent granite.[17]

Calculations of the sort described in reference 3 indicate that with the conditions described above *either* one of the two fractures could provide enough energy for a demonstration heat extraction experiment. Initially, 10 MW (thermal) power could be extracted, but the power would decline in a short period of time (∿ months). A relatively fast drawdown of power is actually preferred, since this results in cooler rock temperatures, with subsequent contraction and cracking of the rock, and, hopefully,enhancement of the heat transfer area. Field measurements of the effects of thermal stress cracking are particularly desirable, since at present, we have available only the theoretical results of Harlow and Pracht[2] to guide us in the design of high performance (∿ 100 MW(t) for ∿ 30 years) reservoirs which continuously grow due to thermal stress cracking.

Unfortunately, a 10 MW (thermal) demonstration heat extraction experiment would require a flow rate of 15 liters/second (240 gal/min) so that even if the present total circulation impedance was approximately 10 bar-sec/ℓ (9 psi-min/gal) as a result of very high permeability, the pressure loss would be 150 bars (2200 psi). This is not realistic since the injection wellbore would be pressurized above the fracture extension pressure while the other would be operated at low pressure, with a lower permeability and higher impedance effect.

Flow Impedance. The explanation we have offered for the observed impedance behavior is a simple one, and therefore appealing. Nature is not often so simple however, and therefore other theories can rightfully be proposed. One alternative theory maintains that flow communication is by means of two intersecting fractures and that the observed flow impedance is primarily due to fractures which are collapsed or nearly closed.

The fractures can stay closed, near the wellbore even at pressures above S_3 because of stress concentrations at the wellbore. Changes in impedance are effected by pressurizing the fractures, forcing them to open somewhat. Such a theory is not in accord with the observed transient pressure data, which depends, for its validity, upon an infinite conductivity fracture; unless it is assumed that the permeability in question is not that of the rock, but that of the fracture. If the latter case were true, then one calculates from the apparent $(A\sqrt{k})_o$ of the fracture, that the fracture aperture must be so large that it should be considered to have an infinite hydraulic conductivity compared to the granite rock. Unfortunately, there are enough uncertainties that these calculations cannot be performed with complete confidence and it is difficult to unequivocally verify one model or the other.

Propping the fractures open with suitable particles, which have high strength and are resistant to 200°C water, is being considered as a technique for reducing the flow impedance. An alternate possibility is chemical treatment with an aqueous solution of sodium carbonate (Na_2CO_3) to preferentially dissolve the quartz component of the granite reservoir and thus increase the rock matrix permeability and fracture conductance and hopefully reduce the total impedance. Should neither of these techniques work, a redrilling operation to actually intersect one of the fractures will be necessary.

CONCLUSIONS:

Two vertical hydraulic fractures have been created in hot, dry granite. The fracture initiated from the EE-1 borehole has been extended on several occasions so that presently both fractures are approximately 90 m (300 ft) or more in radius. In situ measurements of the effect of pore pressure upon rock permeability confirm, qualitatively, laboratory studies on core specimens, and suggest that large increases in permeability occur as the pore pressure approaches the intermediate principal earth stress, S_2.

The two horizontal principal stresses, S_2 and S_3, differ only by 14 bars (200 psi), but they both differ considerably from the vertical stress; so that lithostatic conditions do not prevail at this depth, at this site.

Both fractures are situated deep enough (2.8 km) so that the rock temperature exceeds 185°C (364°F), high enough to be useful for energy extraction. The in situ thermal conductivity is 3 W/mK (1.7 BTU/hr-ft-°F) which compares favorably with laboratory measurements on competent granite core specimens. This combination of favorable rock temperatures, thermal conductivity and fracture radii is sufficient that either fracture could serve as a demonstration heat extraction experiment. Before this is accomplished however, the borehole which is not directly connected to the chosen fracture will have to be cemented off and redrilled so as to directly intersect the fracture selected for exploitation; or else further stimulation (propping or leaching) will be required to attain a low impedance path between the two fractures, in which case heat can be extracted from parts of both fractures. The latter situation may be more advantageous, since, with thermal fracturing, this system may evolve more quickly into one in which heat is being removed by the water from a rock volume, rather than a planar fracture.

NOMENCLATURE:

A = Area (both sides) of fracture
a = wellbore radius
c = specific heat capacity at constant pressure of the rock
c_f = specific heat capacity at constant pressure of the water
E = Young's modulus of elasticity for the rock
$\bar{G}$ = "effective average" water temperature gradient
k = permeability of rock
P = pressure change in the fracture
P_e = fracture extension pressure
q = volumetric flow rate entering the fracture
r = radius coordinate
R = maximum fracture radius
S_1, S_2, S_3 = maximum, intermediate and minimum compressive earth stress, respectively
T = rock temperature
T_f = water temperature
T_{of} = initial (before start of flow) water temperature
t = time
U = velocity of water in the wellbore
z = depth
α = thermal diffusivity of rock ($=\lambda/\rho c$)
$\bar{\beta}$ = mean compressibility ($=\phi\beta_f + (1-\phi)\beta_r$)
β_r = compressibility of rock
β_f = compressibility of water
κ = hydraulic diffusivity ($= k/\mu\bar{\beta}$)
γ = fracture surface energy
λ = thermal conductivity of rock

μ = viscosity of water
ν = Poisson's ratio
ρ = density of rock
ρ_f = density of water
τ = dummy variable of integration
ϕ = porosity
Φ, Ψ = functions of nondimensional groupings

ACKNOWLEDGEMENTS:

The results reported are based upon field testing, which would not have been possible without the efforts of B. Dennis, J. Hill, J. Skalski, E. Stephani, J. Archuleta, E. Horton, B. Todd, D. Yates, C. Fink, and R. Housel. This work was supervised by M. C. Smith whose leadership and dedication to the cause of hot dry rock geothermal energy is gratefully acknowledged.

REFERENCES:

1. Smith, M. C., Aamodt, R. L., Potter, R. M., and Brown, D. W., "Man Made Geothermal Reservoirs" Second United Nations Geothermal Energy Symposium, San Francisco, May 19-29, 1975.
2. Harlow, F. H. and Pracht, W. E. "A Theoretical Study of Geothermal Energy Extraction" J. Geophys. Res. (1972), 77, 7038-7048.
3. McFarland, R. D. and Murphy, H. D. "Extracting Energy from Hydraulically-fractured Geothermal Reservoirs" Eleventh Intersociety Energy Engineering Conference, State Line, Nevada, Sept. 12-17, 1976.
4. Russell, D. G. and Truitt, N. E. "Transient Pressure Behavior in Vertically Fractured Reservoirs" J. Petr. Tech. (Oct. 1964) 1159-1170.
5. Gringarten, A. C., Ramey, H. J., Jr.,and Raghavan, R. "Unsteady-State Pressure Distribution Created by a Well With a Single Infinite-Conductivity Vertical Fracture" Soc. Petr. Engr. Jour. (Aug 1974), 347.
6. ASME Steam Tables (1967)
7. Potter, J. M., Balagna, J. R., and Charles, R. W.: "Permeability of Granitic Rock at Elevated Pressures and Temperatures," Los Alamos Scientific Laboratory report (to be published).
8. West, F. G., Kintzinger, P. R., and Purtyman, W. D.: "Hydrologic Testing Geothermal Test Hole No. 2," Los Alamos Scientific Laboratory report LA-6017-MS, Los Alamos, NM, July 1975.
9. Albright, J. M.: "Preliminary Seismic Mapping of the Main Fracture in GT-2" Abstract published in EOS, 87 (April 1976), No. 4,349.
10. LASL Hot Dry Rock Geothermal Project and Report, 7/1/75 to 6/30/76 (to be published).
11. Sack, R. A.: "Extension of Griffith's Theory of Rupture to Three Dimensions" Proc. Phys. Soc. of London (1946) 58, 729.
12. Aamodt, R. L.: "An Experimental Measurement of In Situ Stress In Granite by Hydraulic Fracturing" Los Alamos Scientific Laboratory report LA-5605-MS, Los Alamos, NM, April 1974.
13. Brace, W. F., Walsh, J. B., and Frangos, W. T. "Permeability of Granite Under High Pressure" J. Geophys. Res. (1968) 73, 2225-2236.
14. Murphy, H. D. and Lawton, R. G.: "Analysis of Temperature Logs in Flowing Geothermal Wells," Los Alamos Scientific Laboratory report in preparation, Los Alamos, NM.
15. Lawton, R. G.: "Welbor: A Transient Heat Transmission Computer Program for a Flowing Well," Los Alamos Scientific Laboratory report in preparation, Los Alamos, NM.
16. Ramey, H. J., Jr.: "Short Term Well Test Data Interpretation in the Presence of Skin Effect and Wellbore Storage," J. Petr. Tech. (Jan 1970) 97-104.
17. Sibbitt, W. L.: "Preliminary Measurements of the Thermal Conductivity of Rocks from LASL Geothermal Test Holes GT-1 and GT-2," Los Alamos Scientific Laboratory report LA-6199-MS, (Jan 1976), Los Alamos, NM.

FIGURES:

Fig 2

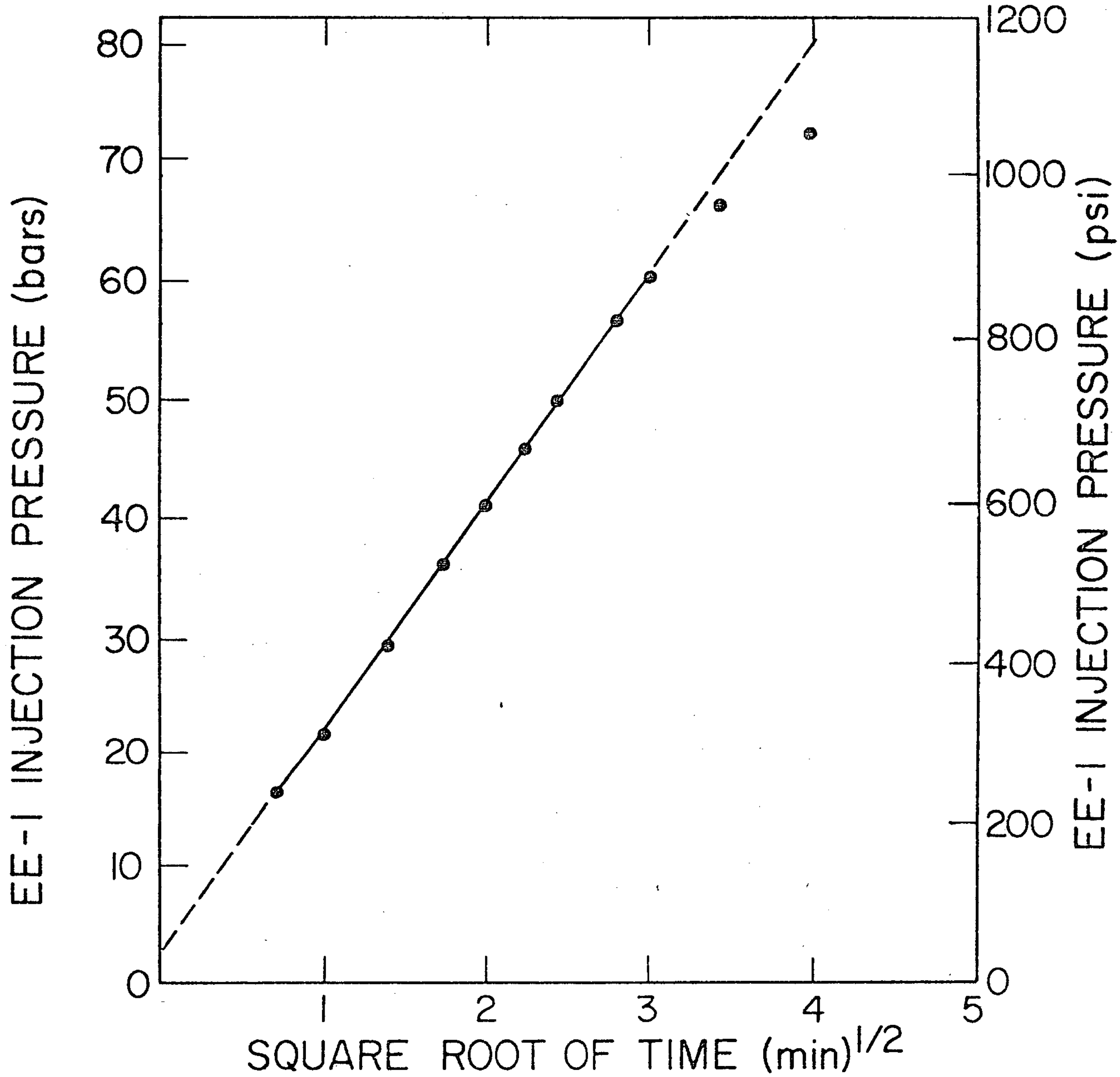

EE-I INJECTION PRESSURE (bars)
80
70
60
50
40
30
20
10
0
1200
1000
800
600
400
200
0
EE-I INJECTION PRESSURE (psi)
1
2
3
4
5
SQUARE ROOT OF TIME (min)$^{1/2}$

Fig 2

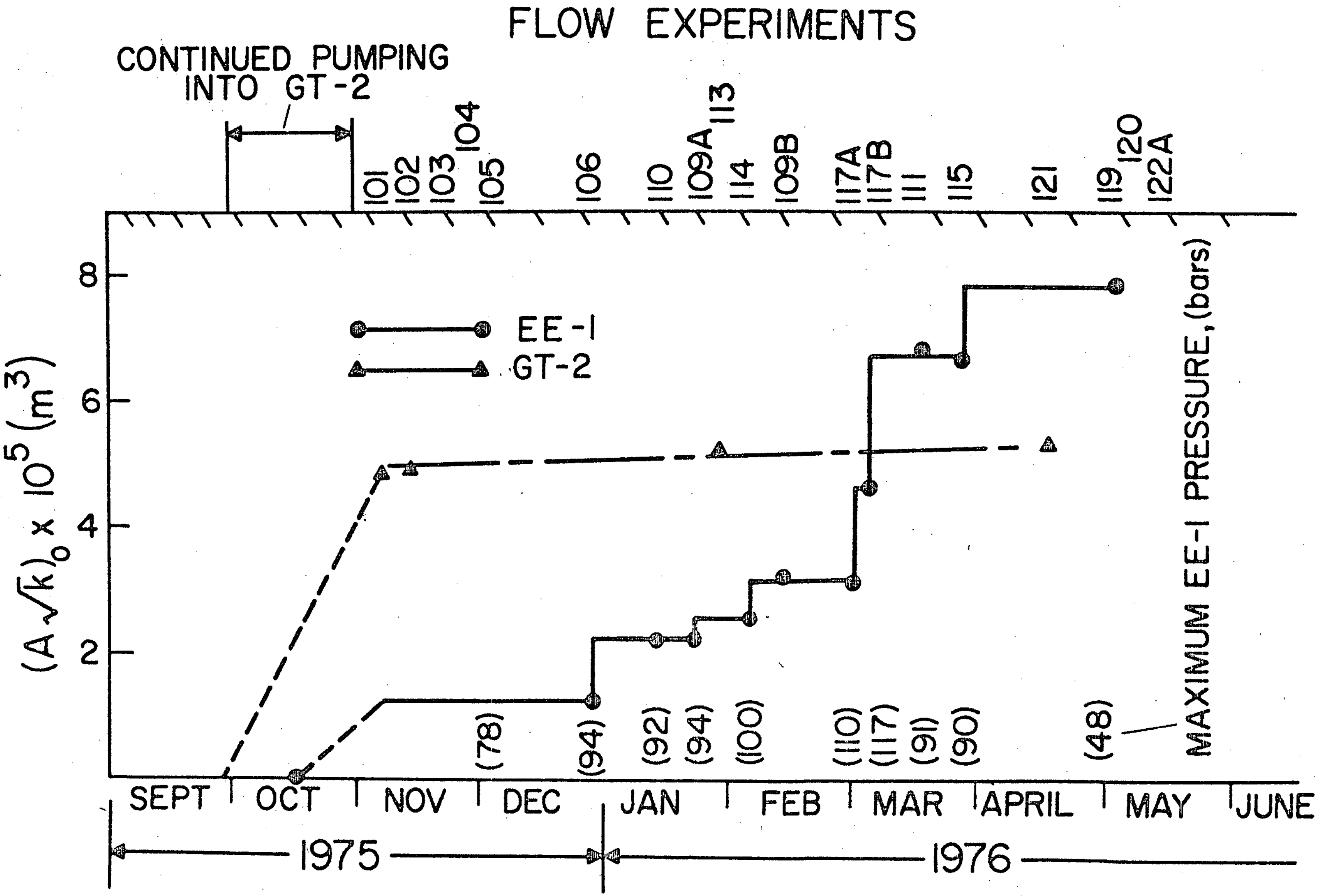

FLOW EXPERIMENTS
CONTINUED PUMPING INTO GT-2
101
102
103
104
105
106
110
109A
113
114
109B
117A
117B
111
115
121
119
120
122A
EE-1
GT-2
$(A\sqrt{k})_o \times 10^5 (m^3)$
8
6
4
2
(78)
(94)
(92)
(94)
(100)
(110)
(117)
(91)
(90)
(48)
MAXIMUM EE-1 PRESSURE, (bars)
SEPT
OCT
NOV
DEC
JAN
FEB
MAR
APRIL
MAY
JUNE
1975
1976

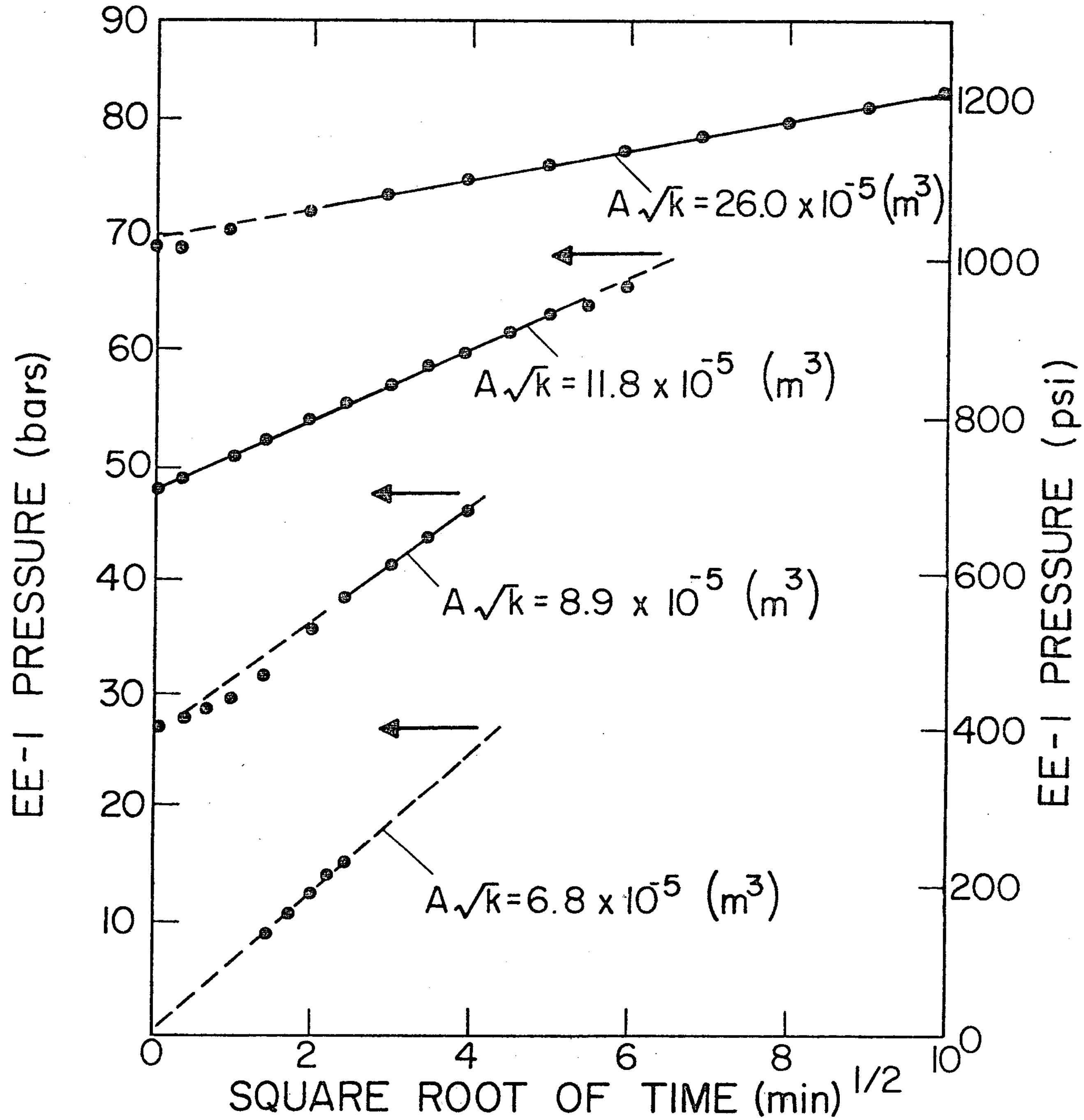

EE-I PRESSURE (bars)
EE-I PRESSURE (psi)
SQUARE ROOT OF TIME (min) 1/2
A √k = 26.0 x 10-5 (m3)
A √k = 11.8 x 10-5 (m3)
A √k = 8.9 x 10-5 (m3)
A √k = 6.8 x 10-5 (m3)
90
80
70
60
50
40
30
20
10
1200
1000
800
600
400
200
0
0
2
4
6
8
10

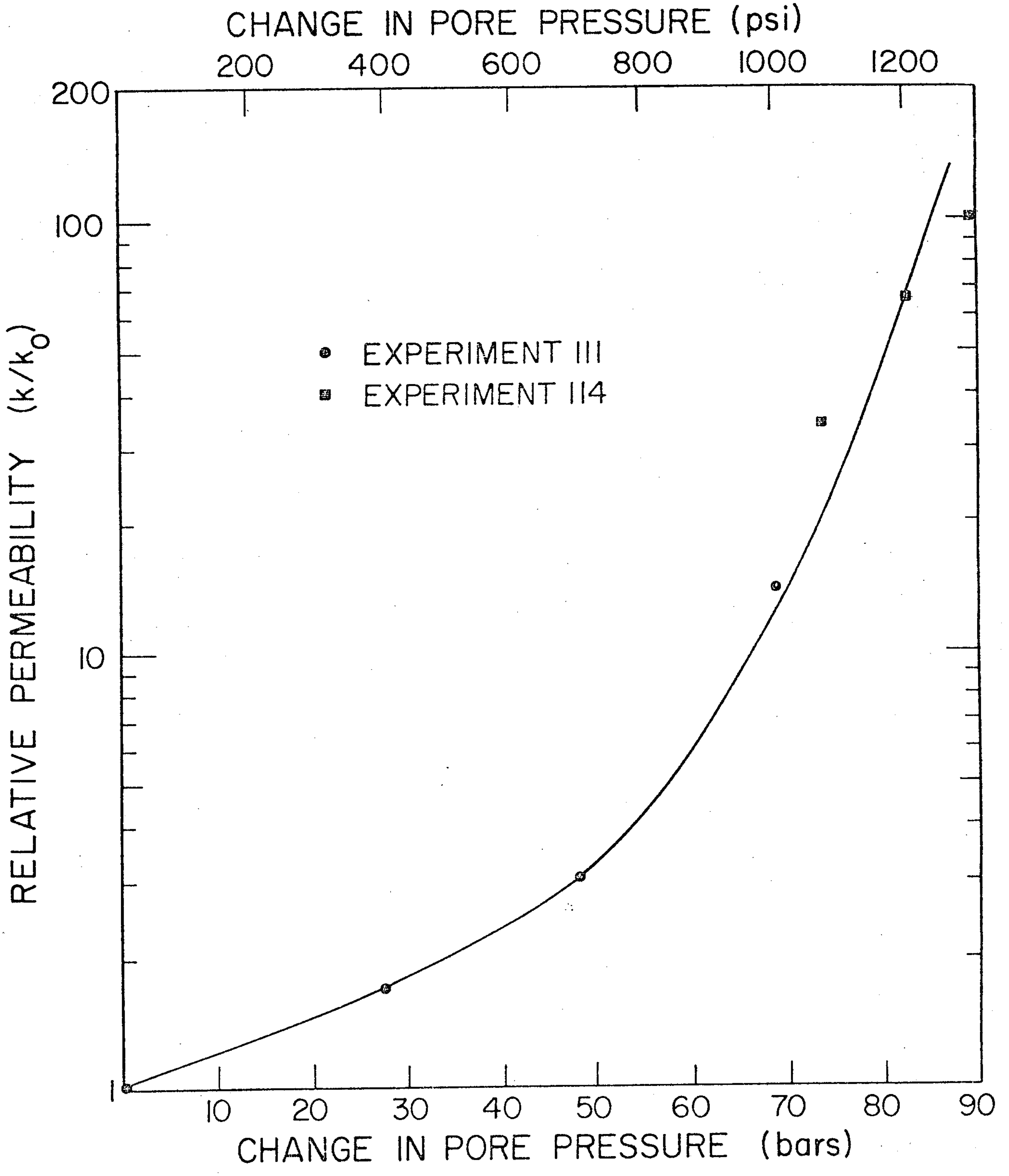
CHANGE IN PORE PRESSURE (psi)
200
400
600
800
1000
1200
200
100
10
1
RELATIVE PERMEABILITY (k/k_o)
EXPERIMENT 111
EXPERIMENT 114
10
20
30
40
50
60
70
80
90
CHANGE IN PORE PRESSURE (bars)

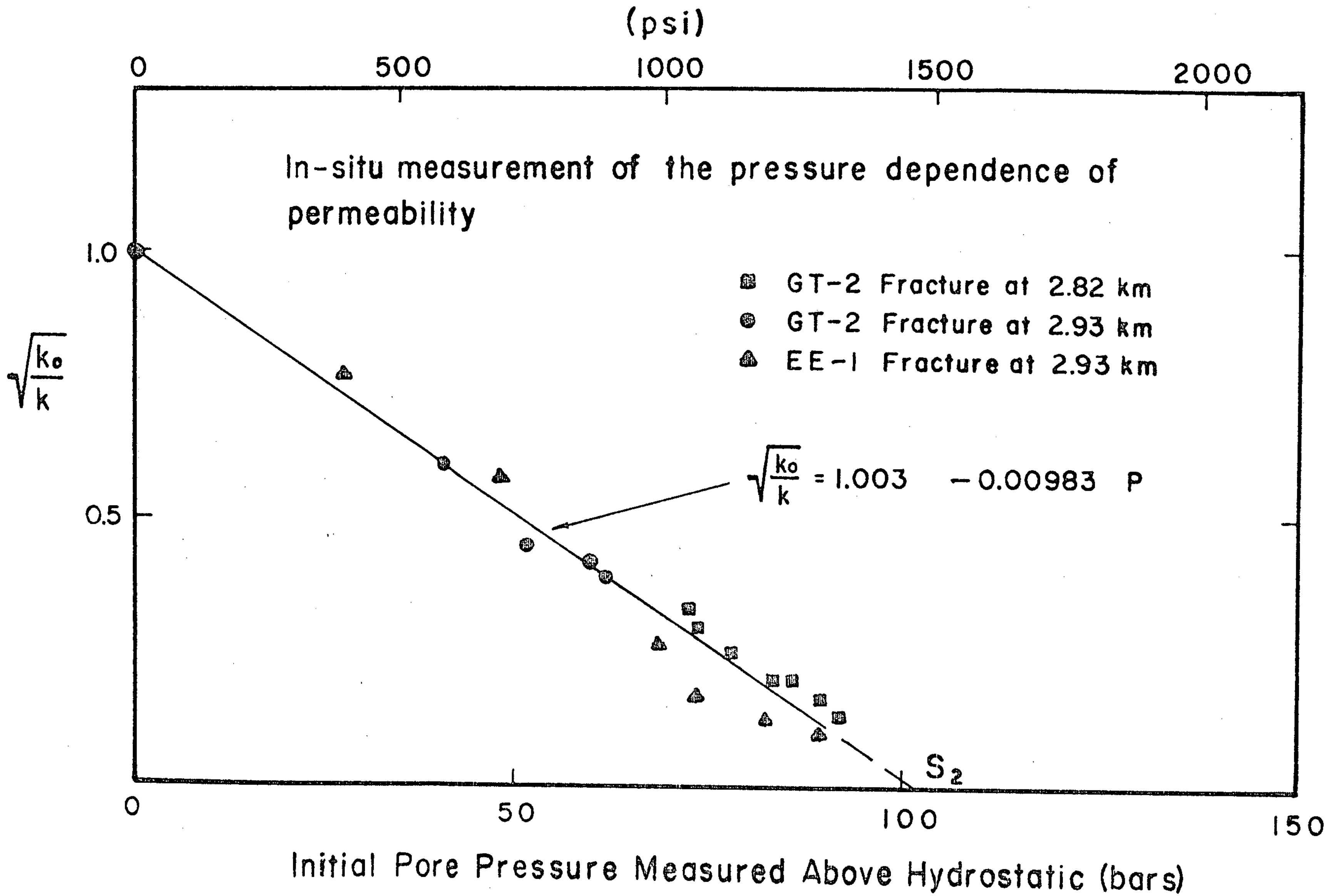

(psi)
0
500
1000
1500
2000
In-situ measurement of the pressure dependence of permeability
1.0
0.5
$\sqrt{\frac{k_o}{k}}$
GT-2 Fracture at 2.82 km
GT-2 Fracture at 2.93 km
EE-1 Fracture at 2.93 km
$\sqrt{\frac{k_o}{k}} = 1.003 - 0.00983 P$
S_2
0
50
100
150
Initial Pore Pressure Measured Above Hydrostatic (bars)

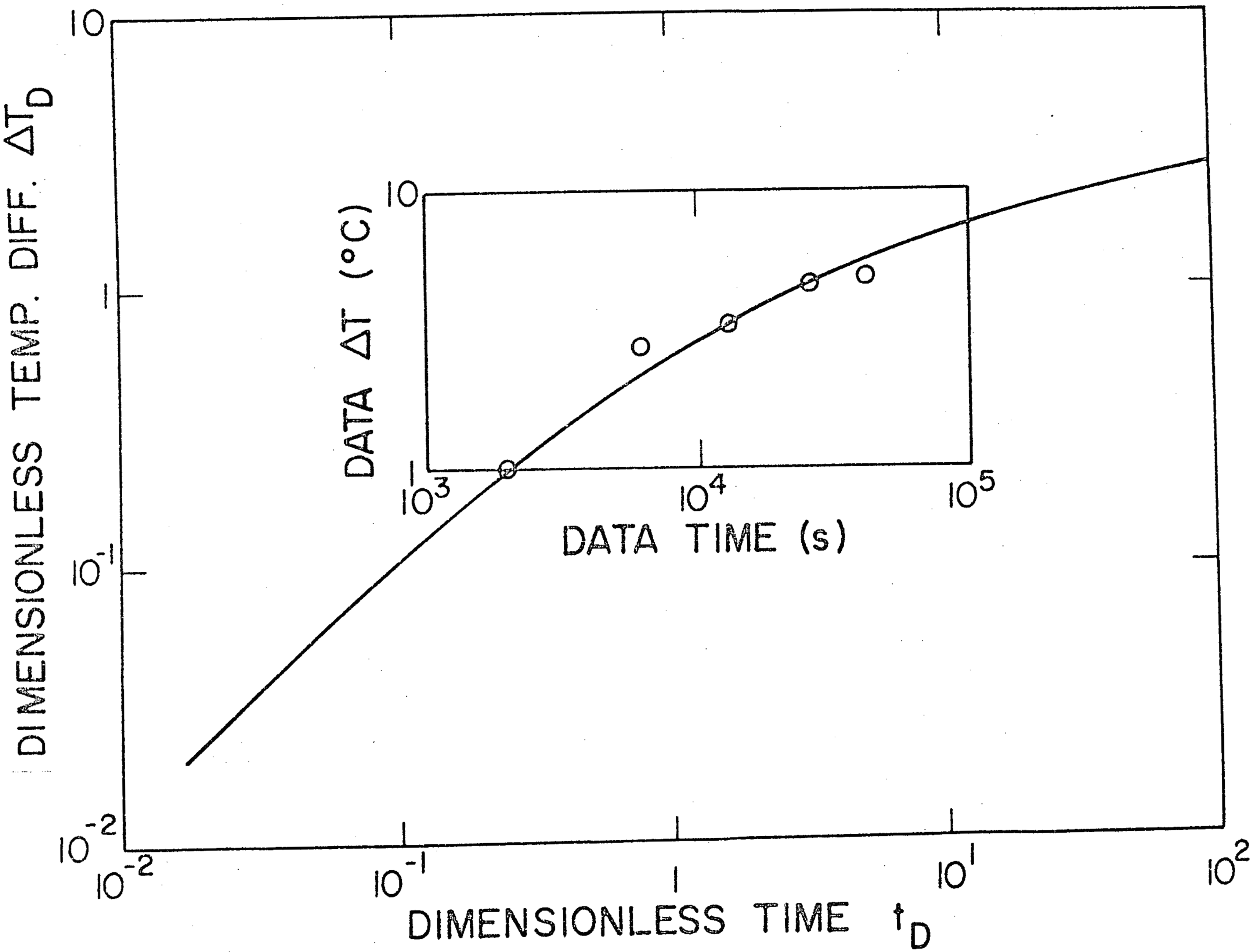

10
1
10⁻¹
10⁻²
10⁻²
10⁻¹
1
10¹
10²
DIMENSIONLESS TEMP. DIFF. ΔT_D
DIMENSIONLESS TIME t_D
10
1
10³
10⁴
10⁵
DATA ΔT (°C)
DATA TIME (s)

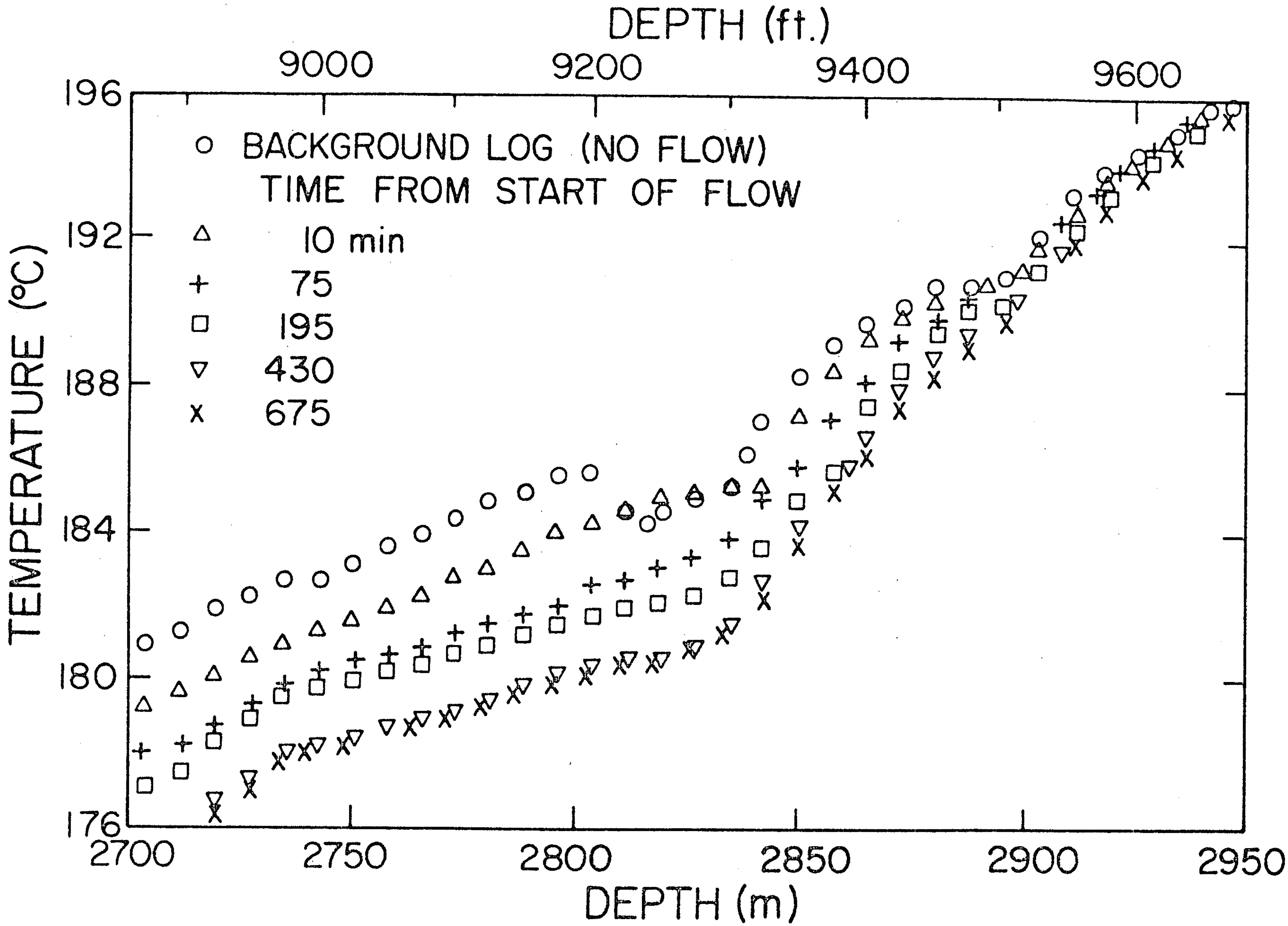
DEPTH (ft.)
9000
9200
9400
9600
196
192
188
184
180
176
TEMPERATURE (°C)
BACKGROUND LOG (NO FLOW)
TIME FROM START OF FLOW
10 min
75
195
430
675
2700
2750
2800
2850
2900
2950
DEPTH (m)

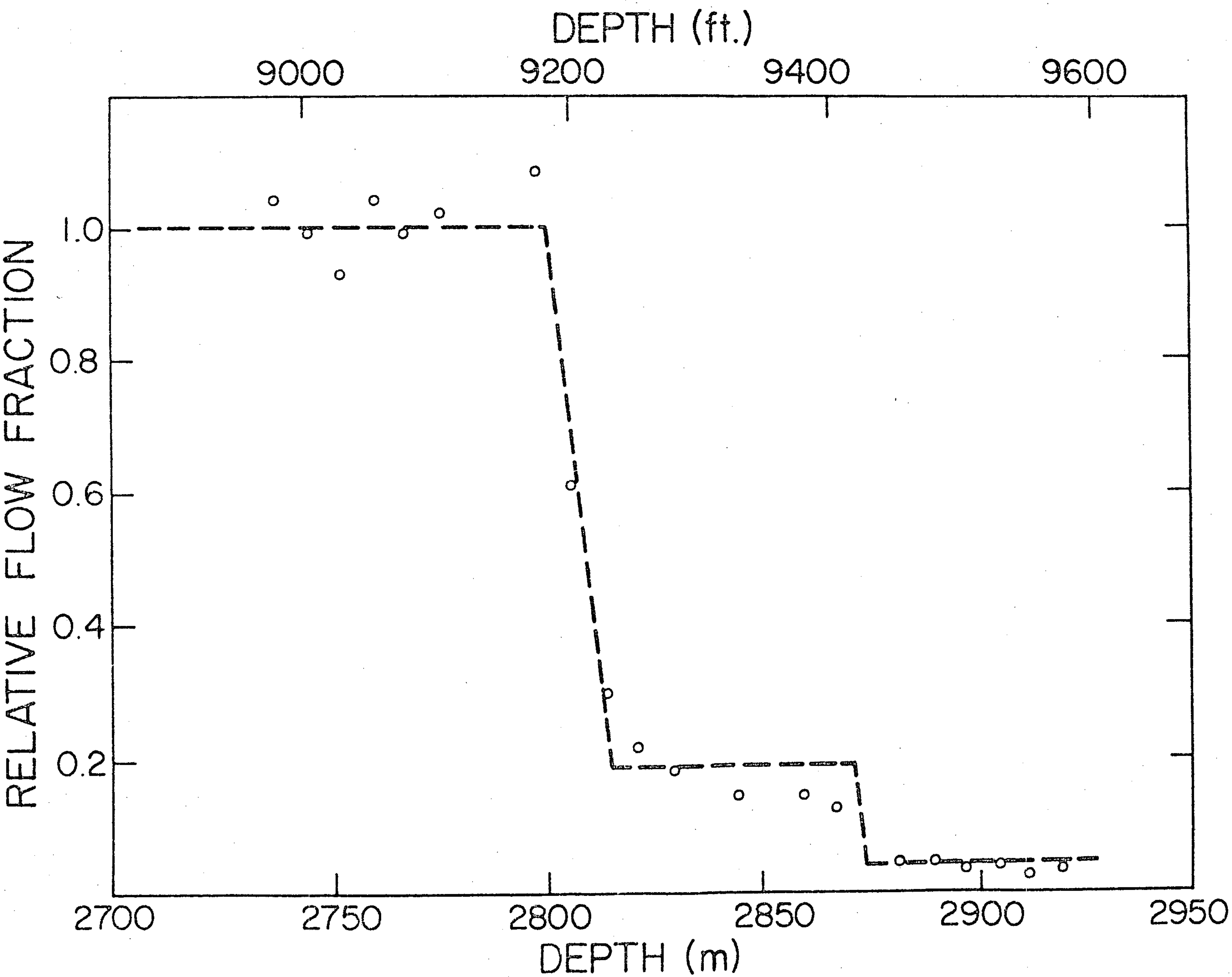

DEPTH (ft.)
9000
9200
9400
9600
RELATIVE FLOW FRACTION
1.0
0.8
0.6
0.4
0.2
2700
2750
2800
2850
2900
2950
DEPTH (m)

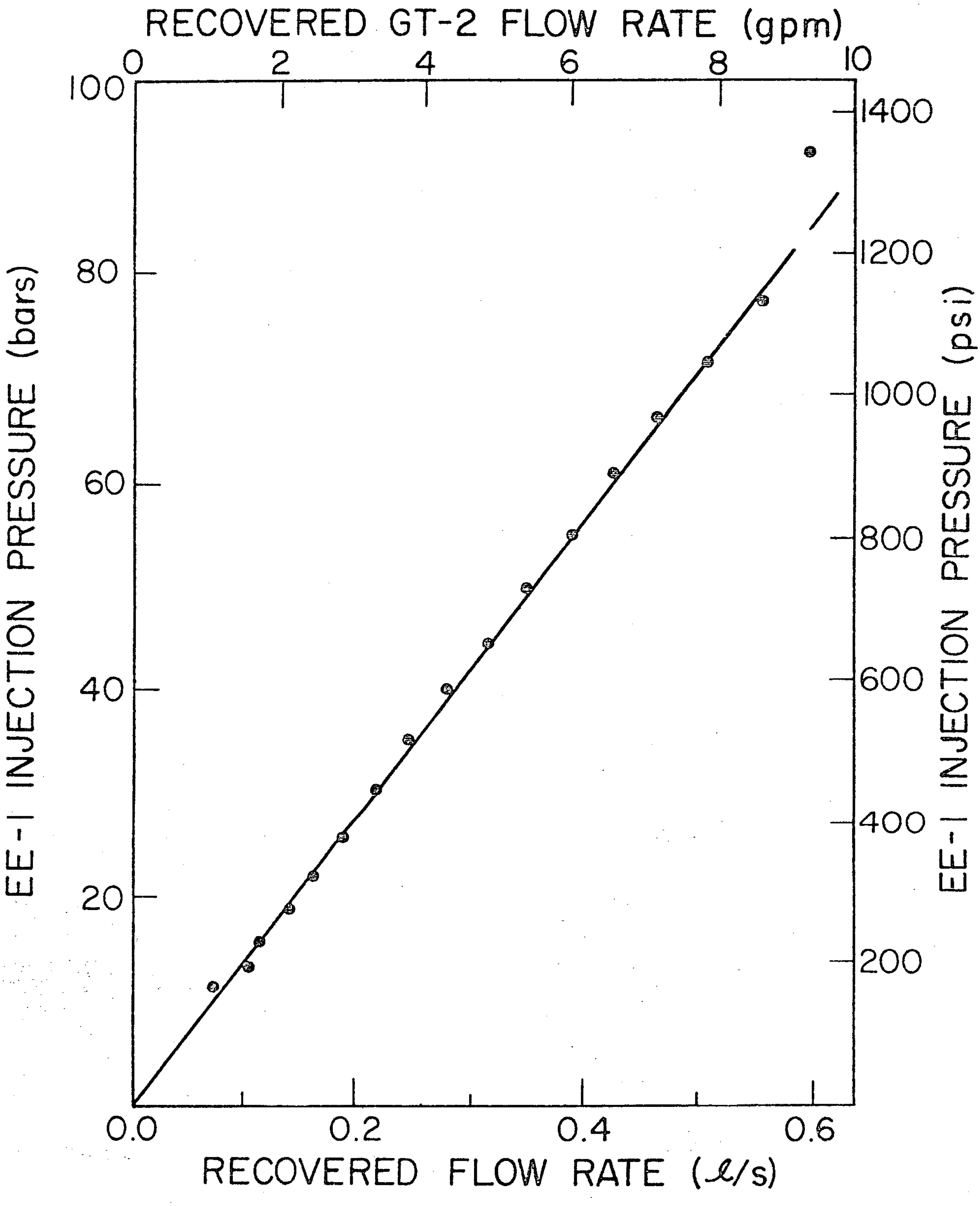
RECOVERED GT-2 FLOW RATE (gpm)
0
2
4
6
8
10
100
80
60
40
20
EE-I INJECTION PRESSURE (bars)
1400
1200
1000
800
600
400
200
EE-I INJECTION PRESSURE (psi)
0.0
0.2
0.4
0.6
RECOVERED FLOW RATE (ℓ/s)

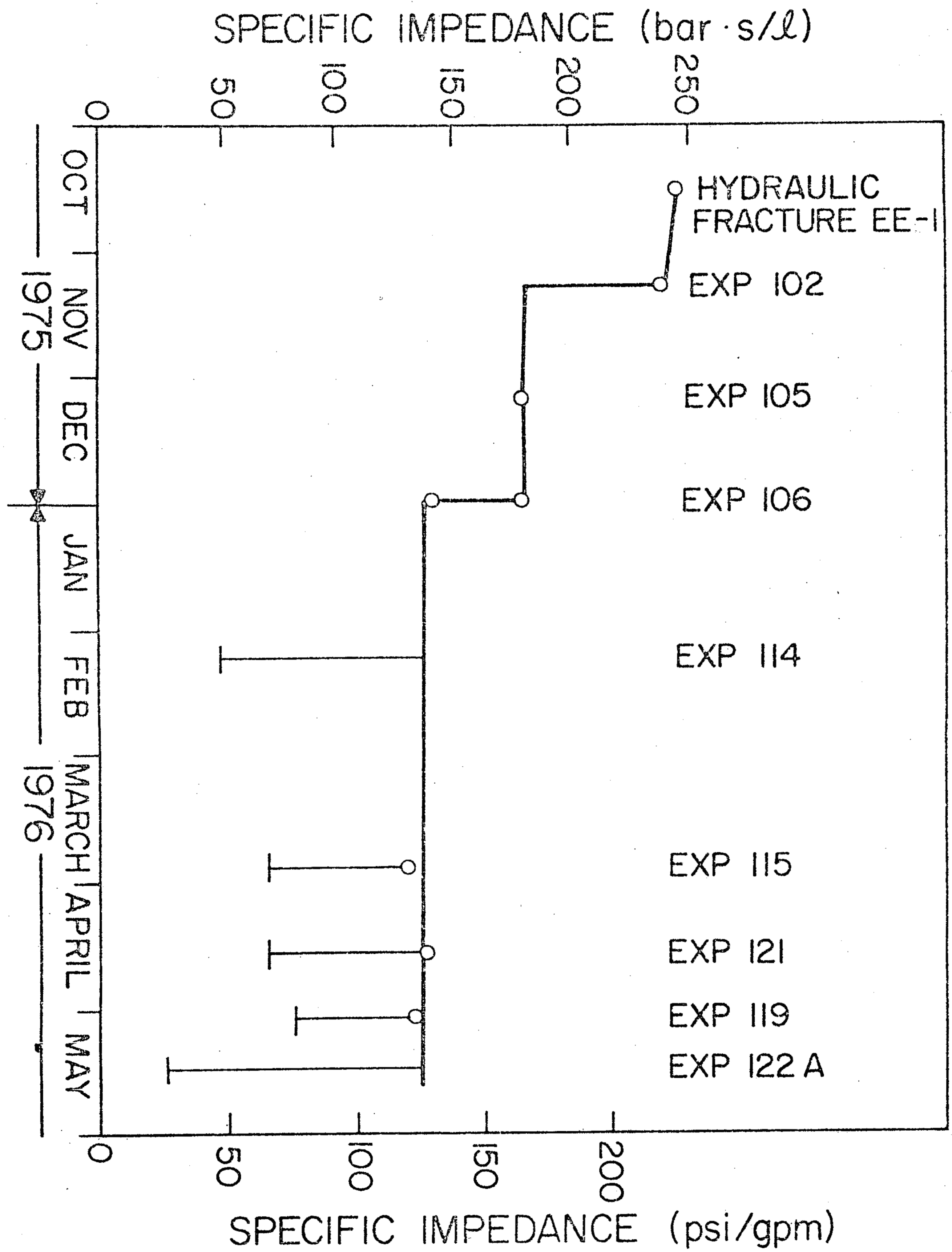
SPECIFIC IMPEDANCE (bar · s/ℓ)
0
50
100
150
200
250
OCT
NOV
DEC
JAN
FEB
MARCH
APRIL
MAY
1975
1976
HYDRAULIC FRACTURE EE-1
EXP 102
EXP 105
EXP 106
EXP 114
EXP 115
EXP 121
EXP 119
EXP 122 A
0
50
100
150
200
SPECIFIC IMPEDANCE (psi/gpm)